

の構成因子(ERK1/2)のリン酸化が亢進していることが分かった。これらの結果は、このシグナル伝達経路の下流にシノビオリンが存在することを示唆する。

他方、RA に比べて OA 優位に転写誘導されている遺伝子群 (OA>R と仮称) はごく少数しか単離・同定できなかった。同じように実験したにも関わらず、RA 優位に転写誘導されている遺伝子が多数単離・同定できたのに、RA に比べて OA 優位に転写誘導されている遺伝子群はほとんど見つからなかったという結果は、少なくとも骨髓液細胞においては発現抑制による機能喪失 (loss of function) よりも過剰発現による機能獲得 (gain of function) が RA の発症において重要な役割を果たすことを示唆する。

D. 考察

これまで単離してきた AURA 遺伝子群の多くは、これまで RA との関連がほとんど研究されていない遺伝子である。そのため、ここで単離・同定した遺伝子群は今後の RA 発症機序の研究の足がかりとして役立つことが示唆される。とくに AREG の過剰発現系は滑膜細胞の過剰増殖に直接の原因となる可能性が示唆された。さらにまだ未解析の AURA 遺伝子の中にも慢性関節リウマチの病因候補として重要な遺伝子も潜んでいる可能性があると考えられる。

E. 結論

本研究計画で進めてきた集約型 DNA マイクロアレイを援用した段階的サブトラクション法による AURA 遺伝子群の単離・同定と機能解析は RA 病因探索の研究に新たな視点を与える可能性が高いと結論した。

F. 健康危険情報

とくになし。

G. 研究発表

1. 論文発表

- (1) 野島 博: DNA 診断と RNA 診断、応用物理、74(10): 1371-1378, 2005.
- (2) Ishii, T., Onda, H., Tanigawa, A., Ohshima, S., Fujiwara, H., Mima, T., Katada, Y., Deguchi, H., Suemura, M., Miyake, T., Miyatake, K., Kawase, I., Zhao,

H., Tomiyama, Y., Saeki, Y., and Nojima, H.: Isolation and expression profiling of genes upregulated in the peripheral blood cells of systemic lupus erythematosus patients. DNA Res., 112(1): 1-11, 2006.

2. 学会発表

なし

H. 知的財産権の出願・登録状況

1. 特許取得

- 1) 血管炎 (angiitis) 患者の血液細胞特異的遺伝子群 (特願 2005-161681)
【発明者】野島博、恩田弘明、橋本博史、小林茂人、鈴木和男
【出願者】科学技術振興機構、大阪大学知財部
【出願日】平成 17 年 6 月 1 日
- 2) 正常ヒト肝臓細胞特異的遺伝子群 (特願 2005-192707)
【発明者】野島博、恩田弘明、門田守人、左近賢人
【出願者】科学技術振興機構、大阪大学知財部
【出願日】平成 17 年 6 月 30 日
- 3) 自己免疫性血小板減少性紫斑病 (ITP) 患者の血液細胞特異的遺伝子群 (特願 2005-306409)
【発明者】野島博、恩田弘明、富山佳昭
【出願者】科学技術振興機構、大阪大学知財部
【出願日】平成 17 年 9 月 30 日

2. 実用新案登録

なし。

3. その他

なし。

D) リウマチ医療体制実態調査研究

厚生労働科学研究費補助金（免疫アレルギー疾患予防・治療研究事業）
分担研究報告書

「関節リウマチ・骨粗鬆症の重症化防止治療開発研究」班
リウマチ施設 診療事例に関する研究

分担研究者 龍 順之助（日本大学医学部整形外科 主任教授）

研究要旨：関節リウマチの診療の現状、病診連携の状況、診療現場での問題点を明らかにするために、全国主要リウマチ施設にアンケート調査を行った。その結果、リウマチ診療にあたる医師の不足、病診連携、各科の連携の向上の必要性、問題点が明らかとなった。今後、リウマチ患者の長期的経過を把握するための全国レベルなどのいくつかの統一したデータベースの作成と管理が必要であることが明らかとなった。

A. 研究目的

関節リウマチ診療現場の問題点を明らかにし、今後どのようにそれらの問題点を解決してゆくべきかについて検討した。特に、各施設のリウマチ診療状況の把握、病診連携の現状、診療現場における問題点と解決策を各施設に報告を依頼し、リウマチ診療現場の事例集を作成した。

B. 研究方法

各診療施設における関節リウマチ診療の現状と問題点、そして今後各施設として、あるいは行政体制として変えてゆくべき方向につき報告することを主な施設に依頼した。

内容として、1) 各施設での診療現況、2) 各施設からの診療連携の状況、3) 各施設での診療実態の問題点、4) 患者の長期経過観察に必要な診療情報をどのように管理しているか、などについての報告を依頼した。

（倫理面への配慮）

本研究においては、特に個人の名前など含まれておりませんので、問題ないと思います。

C. 研究結果

全国より、主要なリウマチ関連施設より、合計 31 件の報告を受領した。施設所在地より、事例を北から南の順に配列し、冊子及び CD-ROM を作成した。その結果、

- 1) リウマチ性疾患の診療状況においては、多くの施設で特に外来において、医師 1 人当たり診察する患者数が多く、実際の診療には患者 1 人 15～20 分程度で十分な時間がとれない現状がある。そのため医師の教育、研究の時間に制限を生じている。
- 2) 診療の連携については、各施設とも内科系及び整形外科との連携をとる方針としている所が多く、外科的手術の適応の有無、また肝臓、腎臓、呼吸器等の合併症につき各科に依頼し連携をとっている。しかし、各科の連携が不十分である施設も少なくない。又、かかりつけ医との病診連携についても、各施設で各医師会や個々の診療施設との連携をとり診療を行っているが、連携が不十分である点も指摘されている。
- 3) 問題点と改善対策 病診連携の問題点として、診療所側はコントロールがうまくゆ

かない患者や手術の患者を紹介するが、患者がある程度落ち着いても、診療所に戻らない、という指摘がある。一方、専門病院側より見ると、紹介のタイミングが遅すぎ、病状が進行し、合併症も生じて依頼されるケースが多い。また手術の依頼に関しても病状が進行し、複雑な手技が必要になることも少なくないことが挙げられる。

4) リウマチ患者の長期経過観察の対策

各施設で診療録の統一とともに患者のデータベースを作成し、臨床検査値、使用薬剤、副作用、画像などさまざまなデータを盛り込み、保存しているケースが多い。今後、情報管理を膨大なデータベースとして処理できる電子カルテのシステムが国にとって必要であろう。

D. 考 察

各問題点につき検討する。

1) リウマチ専門医の育成

各診療所の最大の問題点として、リウマチ患者の数に対して、医師の数が圧倒的に少ないことが挙げられている。1人の医師が複数の患者を診なければならぬため、個々の患者の診察時間が短い現状である。その改善策として、リウマチに興味のある若い医師の教育、育成、リウマチ専門医の増加、特にリウマチ研修施設は継続性のある研修プログラムを作成し、全国の研修希望者を公募するなどの対処が必要である。

またリウマチ学の社会貢献や重要性を学生や研修医に教育、啓発することで、リウマチ医師不足の解消に努めることが求められる。

2) 院内の各科間の連携不足について

各科連携をとり、カンファレンスや症例検討などの機会を設けることが重要である。また薬剤の副作用などで他科を受診するこ

とも少なくないため、リウマチ専門医でない一般医師も、ある程度の関節リウマチに対する知識が必要とされる。そのために、各学会、講演会などで一般の医師に対して、リウマチに対する知識の啓発を行うことが重要である。

3) 地域医療連携について

リウマチ専門施設では、紹介された患者の病状が安定し、治療方法が一定化した場合、紹介された施設は、紹介した施設に返送として診療所に患者を戻すべきであろう。専門施設への患者依頼のタイミングについては、医学情報を十分供給する努力を行い、どの時点で外科的な治療を行うか手術のタイミングを内科医にも知らせる必要がある。また、患者を専門施設に紹介する場合、診療所で手に負えなくなって紹介するのではなく、もう少し早い段階で紹介すべきである。このように、病診連携を相互に推進するために講習会・セミナーなどで、患者紹介のタイミング、手術適応のタイミングなどを周知する機会を持つことが必要である。

4) 診療録の管理について

各施設の報告によれば、各施設でそれぞれの努力をし、診療録をデータベース化して保存している。今後、長期管理をするために、全国共通の一定のデータベースを作成し、各地方のセンターなどに登録システムを作る。さらに電子カルテなども採用し、最終的には全国的なレベルでのデータベースを作成し、リウマチ患者の全国登録を作成する必要がある。

E. 結 論

各リウマチ診療施設の診療の現状、医療連携、リウマチ診療における問題点とその解決策、長期経過観察とそのデータ保存方法につき報告

を依頼した。その結果を冊子にまとめ、CD-ROM
化した。日本におけるリウマチ診療の現状の一
部と問題点が明らかになった。

G. 研究発表

1. 論文発表

特になし

2. 学会発表

特になし

H. 知的財産権の出願・登録状況

(予定を含む。)

1. 特許取得

特になし

2. 実用新案登録

特になし

3. その他

Ⅲ 研究成果の刊行に関わる一覧表

研究成果の刊行に関する一覧表

書籍

著者氏名	論文タイトル名	書籍全体の編集者名	書籍名	出版社名	出版地	出版年	ページ
大島和也、 下村伊一郎	基礎： アディポサイトカイン Adipocytokine	西沢 良記	骨粗鬆症治療	株式会社 先端医学 社	東京	2005	Vol. 4 no. 4 64-71 (340)
広畑俊成	8. リウマチ・アレルギー性疾患 Behçet病	矢崎義雄、 菅野健太郎	改訂第4版 疾患別最新処方	Medical View社	東京	2005	524-525
広畑俊成	第3部生体防御および病態解析 ・治療の免疫機構 第3章自己 免疫疾患 3.2 病態・診断およ び治療 [1] 全身性エリテマト ーデスの病態および診断 [2] 各種免疫抑制薬の作用機序 [3] 抗体療法を中心とした生物 学的製薬	免疫学 ハンドブック 編集委員会 (垣内史堂、 編集委員長)	免疫学ハンドブック (Immunology handbook)	オーム社	東京	2005	394-398

雑誌

発表者氏名	論文タイトル名	発表誌名	巻号	ページ	出版年
Takaji M, Shiba K, Yoshioka T, Tsuruta Y, Suzuki R, <u>Ochi T</u> , Itoh T, Musha H, Mizoi T, Sasaki I	Evidence for existence of oligoclonal tumor-infiltrating lymphocytes and predominant production of T helper 1/T cytotoxic 1 type cytokines in gastric and colorectal tumors	International Journal of oncology	25	133-141	2004
Takano H, Tomita T, Toyosaki-Maeda T, Maeda-Tanimura M, Tsuboi H, Takeuchi E, Kaneko M, Shi K, Takahi K, Myoui A, Yoshikawa H, Takahashi T, Suzuki R, <u>Ochi T</u> .	Comparison of the activities of multinucleated bone-resorbing giant cells derived from CD14-positive cells in the synovial fluids of rheumatoid arthritis and osteoarthritis patients.	Rheumatology	43(4)	431-441	2004
Hirohata, S., Yanagida, T., Nampei, A., Kunugiza, Y., Hashimoto, H., Tomita, T., Yoshikawa, H., <u>Ochi, T</u>	Enhanced generation of endothelial cells from CD34+ cells of the bone marrow in rheumatoid arthritis: Possible role in synovial neovascularization.	Arthritis and Rheumatism	50	3888-3896	2004
<u>K. Oshima</u> , A. Nampei, M. Matsuda, M. Iwaki, A. Fukuhara, J. Hashimoto, H. Yoshikawa, <u>I. Shimomura</u>	Adiponectin increases bone mass by suppressing osteoclast and activating osteoblast	Biochemical and Biophysical Research Communications	331	520-526	2005

S. Nakamura-Kikuoka, K. Takahi, H. Tsuboi, T. Toyosaki-Maeda, M. Maeda-Tanimura, C. Wakasa, N. Kikuchi, S. Norioka, M. Iwasaki, T. Matsutani, T. Otoh, S. Yamane, H. Takemoto, Y. Tsuruta, Y. Shimaoka, M. Yukioka, <u>R. Suzuki</u> and T. Ochi	Limited VH gene usage in B-cell clones established with nurse-like cells from patients with rheumatoid arthritis	<i>Rheumatology (Oxford)</i> .			2005Dec20 ; [Epub ahead of print]
K. Tanaka, T. Toshihiro, T. Juji, S. Suzuki, J. Watanabe, A. Goto, N. Shiobara, S. Yamane, N. Fukui, <u>R. Suzuki</u> and T. Ochi	Production of interleukin-6 and interleukin-8 by nurse-like cells from rheumatoid arthritis patients after stimulation with monocytes	<i>Mod Rheumatol</i>	15	415-422	2006
T. Tashiro, H. Hirokawa, Y. Ikeda, T. Ohnuki, <u>R. Suzuki</u> , <u>T. Ochi</u> , K. Nakanura and N. Fukui	Effect of GDF-5 on ligament healing	J Orthop Res	24(1)	71-79	2006
鈴木隆二	リウマチの破骨細胞	臨床整形外科	41(3)	260-263	2006
<u>Tanaka S</u> , Takahashi N, Nakamura K, Suda T	Role of RANKL in physiological and pathological bone resorption and therapeutics targeting RANKL-RANK signaling system.	Immunological Review	108	30-49	2005
Fukuda A, Hikita A, Wakeyama H, Akiyama T, Oda H, Nakamura K, <u>Tanaka S.</u>	Regulation of osteoclast apoptosis and motility by small GTPase binding protein Rac1.	J Bone Miner Res	20	2245-2253	2005
Hikita A, Kadono Y, Chikuda H, Fukuda A, Wakeyama H, Yasuda H, Nakamura K, Oda H, Miyazaki T, <u>Tanaka S.</u>	Identification of an alternatively spliced variant of CAPRI as a possible regulator of RANKL shedding.	J Biol Chem	280	41700-41706	2005
野島 博	DNA診断とRNA診断	応用物理	74(10)	1371-1378	2005
Ishii, T., Onda, H., Anigawa, A., Ohshima, S., Fujiwara, H., Mima, T., Katada, Y., Deguchi, H., Suemura, M., Miyake, T., Miyatake, K., Kawase, I., Zhao, H., Tomiyama, Y., Sacki, Y., and Nojima, H.	Isolation and expression profiling of genes upregulated in the peripheral blood cells of systemic lupus erythematosus patients.	DNA Research	112(1)	1-11	2006

Yajima N, Kasama T, Isozaki T, Odai T, Matsunawa M, Negishi M, Ide H, Kameoka Y, Hirohata S, Adachi M	Elevated levels of soluble fractalkine inactive systemic lupus erythematosus. Potential involvement in neuropsychiatric manifestations. hcet病	Arthritis Rheum	52	1670-1675	2005
Shibuya H, Hirohata S	Differential effects of IFN- γ on the expression of various Th2 cytokines in human CD4+ T cells.	J Allergy Clin Immunol	116	123-126	2005
Suzuki F, Nanki T, Imai T, Kikuchi H, Hirohata S, Kohsaka H, Miyasaka N	Inhibition of CX3CL1 (Fractalkine) improves experimental autoimmune myositis in SJL/J mice.	J Immunol	175	6987-6996	2005
広畑俊成	第6回 Latest Orthopedics 研究会の記録. 関節リウマチの病態形成における骨髄異常について.	骨・関節・靭帯	18	257-264	2005
広畑俊成	特集: 痴呆症の最新情報—治せる痴呆を見逃さないために <内科疾患に伴う treatable dementia > 膠原病による痴呆.	内科	95	857-862	2005
広畑俊成	第1土曜特集 Behcet 病—病因の解明と難治性病態の克服に向けて. 神経 Behcet 病の臨床. i	医学のあゆみ	215	61-66	2005
広畑俊成	中枢神経病変.	臨床リウマチ	17	278-282	2005
Miyata, K, Oike, Y, Hoshii, T, Maekawa, H, Ogawa, H, Suda, T, Araki, K, and Yamamura, K.	Increase of smooth muscle cell migration and of intimal hyperplasia in mice lacking the abhydrolase domain containing 2 gene.	Biochem Biophys Res Commun.	329	296-304	2005
Taniwaki, T., Haruna, K., Nakamura, H., Sekimoto, T., Oike, Y., Imaizumi, T., Saito, F., Muta, M., Soejima, Y., Utoh, A., Nakagata, N., Araki, M., Yamamura, K., Araki, K.	Characterization of an exchangeable gene trap using pU-17 carrying a stop codon-beta-geo cassette.	Dev. Growth Differ.	47	163-172	2005
Ohmuraya, M., Hirota, M., Araki, M., Mizushima, N., Matsui, M., Mizumoto, T., Haruna, K., Kume, S., Takeya, M., Ogawa, M., Araki, K. and Yamamura, K.	Autophagic cell death of pancreatic acinar cells in serine protease inhibitor Kazal Type 3 deficient mice.	Gastroenterology	129	696-705	2005
Washington Smoaka, I, Byrdb, N. A., Abu-Issab, R., Goddeerisc, M. M., Andersonc, R., Morrisb, J., Yamamurad, K., Klingens mithe, J., Meyers, E. N.	Sonic hedgehog is required for cardiac outflow tract and neural crest cell development.	Dev. Biol.	283	357-372	2005

Yamazaki, H., Sakata, E., Yamano, T., Yanagisawa, A., Abe, K., Yamamura, K., Hayashi, S. and Kunisada, T.	Presence and distribution of neural crest-derived cells in the murine developing thymus and their potential for differentiation.	Int. Immunol.	17	549-558	2005
Semba, K., Araki, K., Ii, Z., Matsumoto, K., Suzuki, M., Nakagata, N., Takagi, K., Takeya, M., Yoshinobu, K., Araki, M., Imai, K., Abe, K. and Yamamura, K.	A novel murine gene, <i>Sickle tail</i> (<i>Skl</i>), linked to the <i>Danforth's short tail</i> (<i>Scd</i>) locus, is required for normal development of the intervertebral disc.	Genetics	172	445-456	2006
Alex S. Nord, A. S., Patricia J. Chang, P. J., Bruce R. Conklin, B. R., Cox, C., Harper, C. A., Hicks, G. G., Huang, C. C. Johns, S. J., Kawamoto, M., Liu, S., Meng, E. C., Morris, J. H., Rossant, J., Ruiz, P., Skarnes, W. C., Soriano, P., Stanford, W. I., Stryke, D., von Melchner, H., Wurst, W., Yamamura, K., Young, S. G., Babbitt, P. C. and Ferrin, T. E.	The international gene trap consortium web site: a portal to all publicly available gene trap cell lines and mouse.	Nucleic Acids Res.	34	D642-D648	2006
Miura, K., Yoshinobu, K., Imaizumi, T., Haruna, K., Miyamoto, Y., Yoneda, Y., Nakagata, N., Araki, M., Miyakawa, T., Yamamura, K. and Araki, K.	Impaired expression of Importin/karyopherin β 1 leads to post-implantation lethality.	Biochem Biophys Res Commun.	341	132-138	2006
Kishigami, S., Komatsu, Y., Takeda, H., Nomura-Kitabayashi, A., Yamauchi, Y., Abe, K., Yamamura, K. and Mishina, Y.	An optimized beta-gal staining method for simultaneous detection of endogenous gene expression in early mouse embryos.	Genesis	In press		
Ohmuraya, M., Hirota, M., Araki, K., Baba, H. and Yamamura, K.	Enhanced trypsin activity in pancreatic acinar cells deficient for serine protease inhibitor Kazal type 3.	Pancreas	In press		

IV 研究成果の刊行物



Potential of the activity of bone morphogenetic protein-2 in bone regeneration by a PLA–PEG/hydroxyapatite composite

Takashi Kaito^{a,*}, Akira Myoui^a, Kunio Takaoka^b, Naoto Saito^c, Masataka Nishikawa^a, Noriyuki Tamai^a, Hajime Ohgushi^d, Hideki Yoshikawa^a

^a Department of Orthopaedic Surgery, Osaka University Graduate School of Medicine, 2-2 Yamadaoka, Suita, Osaka, 565-0871, Japan

^b Department of Orthopaedic Surgery, Shinshu University School of Medicine, 3-3-1 Asahi Matsumoto, Nagano 390-8621, Japan

^c Department of Orthopaedic Surgery, Osaka City University Graduate School of Medicine, 1-5-7 Asahimachi, Abeno-ku, Osaka 545-0051, Japan

^d Tissue Engineering Research Center (TERC), National Institute of Advanced Industrial Science and Technology (AIST), 3-11-46, Nakoji, Amagasaki, Hyogo 661-0974, Japan

Received 14 December 2003; accepted 3 February 2004

Abstract

Bone morphogenetic proteins (BMPs) are biologically active molecules capable of inducing new bone formation, and show potential for clinical use in bone defect repair. However, an ideal system for delivering BMPs that can potentiate their bone-inducing ability and provide initial mechanical strength and scaffold for bone ingrowth has not yet been developed. In this study, to construct a carrier/scaffold system for BMPs, we combined two biomaterials: interconnected-porous calcium hydroxyapatite ceramics (IP-CHA), and the synthetic biodegradable polymer poly D,L-lactic acid–polyethyleneglycol block co-polymer (PLA–PEG). We used a rabbit radii model to evaluate the bone-regenerating efficacy of rhBMP-2/PLA–PEG/IP-CHA composite. At 8 weeks after implantation, all bone defects in groups treated with 5 or 20 µg of BMP were completely repaired with sufficient strength. Furthermore, using this carrier scaffold system, we reduced the amount of BMP necessary for such results to about a tenth of the amount needed in previous studies, probably due to the superior osteoconduction ability of IP-CHA and the optimal drug delivery system provided by PLA–PEG, inducing new bone formation in the interconnected pores. The present findings indicate that the synthetic biodegradable polymer/IP-CHA composite is an excellent combination carrier/scaffold delivery system for rhBMP-2, and that it strongly promotes the clinical effects of rhBMP-2 in bone tissue regeneration.

© 2004 Elsevier Ltd. All rights reserved.

Keywords: BMP (bone morphogenetic protein); Hydroxyapatite; Drug delivery; Polylactic acid; Bone tissue engineering

1. Introduction

Bone defects due to tumor resection, trauma and congenital abnormality are a great challenge to reconstructive surgery. Autologous bone grafting is a popular procedure, but it has many disadvantages such as limited supply of suitable bone and persistence of pain, nerve damage, fracture and cosmetic disability at the donor site. There are no donor site problems with allografting, but it involves risks of disease transmission and immunological reaction [1]. For these reasons, it is hoped that treatment with bone morphogenetic proteins (BMPs), which belong to the transforming growth

factor (TGF) superfamily and are known to be capable of eliciting new bone formation both orthotopically and heterotopically in experimental animal models, can provide an alternative to bone grafting [2–4]. Three types of BMP-based bone tissue engineering have been tried to date: cell therapy, gene therapy, and cytokine therapy. Cell therapy involves transplantation of autogenous bone marrow mesenchymal cells differentiated by BMP. Gene therapy involves transduction of genes encoding BMPs into cells at the repair site. Cytokine therapy involves recombinant BMP and carriers that retain and release BMP as needed. Cytokine therapy is considered the most promising of these approaches for practical use [5].

In cytokine therapy, the drug delivery system should not only promote effective biological activity but also limit spatial spread of the cytokine as appropriate [6].

*Corresponding author. Tel.: +81-06-6879-3552; fax: +81-06-6879-3559.

E-mail address: t-kaito@leto.eonet.ne.jp (T. Kaito).

Many materials have been evaluated as carriers for BMP, including synthesized polymer, collagen, tricalcium phosphate, and classical hydroxyapatite. Although all of these materials can induce bone formation in ectopic and orthotopic sites, they have not yet gained widespread use because of disadvantages such as risk of disease transmission, fragility, difficulty in handling, lack of porous structures suitable for cell infiltration, and limited supply [7–11].

Another important unresolved issue in BMP-based bone regeneration is the amount of BMP necessary to induce sufficient new bone formation in humans. For example, due to differences in responsiveness to BMP, humans respond to quantities in mg to induce new bone formation, whereas mice, BMP quantities in μg is sufficient [12,13].

To resolve these issues, the present delivery system combines two biomaterials: a three-dimensional interconnected porous scaffold with initial mechanical strength and bone conduction ability, and a biodegradable synthetic polymer that provides sustained release of BMP. The scaffold we chose was a fully interconnected porous calcium hydroxyapatite ceramic (IP-CHA) that we developed using a “foam-gel” technique. Previously, we showed that IP-CHA has superior osteoconduction ability [14]. The carrier we selected was poly D,L-lactic acid–polyethylene glycol block copolymer (PLA–PEG), which is reportedly an effective carrier material for recombinant human BMP-2 (rhBMP-2) [15,16].

This report describes the bone-inducing effects of a PLA–PEG/IP-CHA composite containing a small amount of rhBMP-2, in a rabbit radius segmental defect model.

2. Materials and methods

2.1. Preparation of implants

Cylindrical pieces of IP-CHA (diameter, 4 mm; height, 15 mm) were provided by Toshiba Ceramics Co., Ltd (Kanagawa, Japan). IP-CHA has a well-organized interconnected structure with total porosity of 75% and average interconnection channel diameter of 40 μm . Theoretically, more than 90% of the pores are connected to channels with a diameter greater than 10 μm , allowing tissue invasion from pore-to-pore [14].

The rhBMP-2, which was produced at the Genetics Institute (Cambridge, MA) and donated to us through Yamamouch Pharmaceutical Co., Ltd. (Ibaraki, Japan), was dissolved in a buffer (5 mM glutamic acid, 2.5% glycine, 0.5% sucrose, and 0.01% Tween 80) at a concentration of 1 $\mu\text{g}/\mu\text{l}$.

PLA–PEG with a total molecular weight of 11 400 Da and a PLA:PEG molar ratio of 51:49 was synthesized and provided by Taki Chemicals Co., Ltd (Hyogo, Japan).

The polymer mass was liquidized in acetone and mixed with 5 or 20 μg of rhBMP-2. Next, this mixture was dropped onto the IP-CHA (Fig. 1A), and the acetone was then removed by evaporation in a safety cabinet to return the polymer to its native state.

2.2. Scanning electron microscopy (SEM)

To verify that the pore surface of IP-CHA was coated by rhBMP-2/PLA–PEG homogeneously, the implants were cut into halves across the longitudinal axis and the cut surface was observed with a scanning electron microscope (JSM-6000F, Nihon Denshi Oyo Co., Ltd., Tokyo, Japan).

2.3. Animal experiment

Thirty New Zealand white rabbits weighing an average of 3.5 kg were used. The animals were anesthetized using an intra-venous injection of 50 mg pentobarbital and 25 mg xylazine hydrochloride, together with a subcutaneous injection of 0.5 ml of 1% lidocaine with 0.01% epinephrine around the operative site. An approximately 3-cm-long incision was made, and the tissues overlying the distal diaphyseal radius were dissected. A 1.5-cm segmental osteoperiosteal defect was created in the radius with a mini-oscillating saw. Ten animals each were implanted with rhBMP-2/PLA–

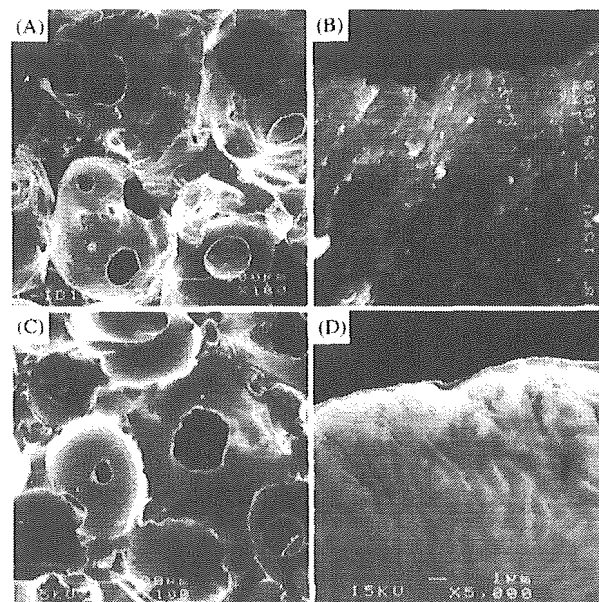


Fig. 1. SEM photographs of IP-CHA before (A,B) and after (C,D) PLA–PEG coating. Magnification: (A,C) $\times 100$; (B,D) $\times 5000$. (A) Large spherical pores (diameter, 100–200 μm) were divided by thin walls and interconnected to one another. (B) Before PLA–PEG coating, individual hydroxyapatite particles were clearly visible. (C) After coating, at lower magnification, interconnecting channels were still clearly visible. (D) At higher magnification, the boundaries between individual hydroxyapatite particles became ambiguous.

PEG/IP-CHA composite containing 5 μg (5 μg BMP group) or 20 μg (20 μg BMP group) of rhBMP-2. These two groups were each subdivided into two subgroups ($n=5$), which were sacrificed at 4 and 8 weeks after implantation, respectively. In five animals (defect group), nothing was implanted in the defect; these animals were sacrificed at 8 weeks. In five animals (IP-CHA alone group), IP-CHA without BMP/PLA-PEG coating was implanted; these animals were sacrificed at 8 weeks. Animals were kept in the Institute of Experimental Animal Sciences (IEXAS), Osaka University Medical School, in accordance with the institutional guidelines for care and use of laboratory animals. Sacrifice was performed by overdose anesthesia, and implanted forearms were harvested together with surrounding tissues.

2.4. Radiographic examination and bone mineral density (BMD)

All harvested tissues were fixed with 10% neutral formalin and then radiographed with a soft X-ray apparatus (MX-20 Faxitron, Torrex and Micro Focus Systems, Wheeling, IL). BMD was determined by dual-energy X-ray absorptiometry (DXA) using an animal densitometer (PIXImus, Lunar Corp., Madison, WI). In scans of the excised bones, the region-of interest (ROI) was positioned over the whole implant area (IP-CHA) on the anterior–posterior view, not including host bone or bone that developed outside the implant. BMD was determined using the image analysis software provided with the instrument.

2.5. Microfocus-computed tomography (CT) and mechanical evaluation

From four animals in each group, two 4-mm-high discs were carved from the center of the cylindrical IP-CHA blocks: one for CT and histological evaluation, and the other for mechanical evaluation. Bone formation in IP-CHA pores was evaluated using a microfocus CT system (MCT-CB100MF(Z); Hitachi Medical Corporation, Tokyo, Japan). After fixation in 10%-buffered formalin, each sample was scanned at intervals of 10 μm , at 50 kV and 200 μA . Analytical conditions were super-precision mode and 7-times magnification, with an image intensifier field of 1.8 in. The radiodensity of the newly formed bone on CT images was determined by comparing the histological section with the corresponding CT image. Then, the newly formed bone area on the CT images was extracted, and its volume was measured using the software package TRI3D-BON (Ratoc System Engineering Co., Ltd., Tokyo, Japan). Compression tests were performed using AUTOGRAPH AG-10KNI (Shimadzu Corp., Kyoto, Japan), with a compression speed of 1 mm/min. Testing was performed vertically

towards the specimen, along the longitudinal axis of the radius.

2.6. Histological evaluation

One of the five tissue samples from each group was demineralized with 50% formic acid and 10% sodium citrate, dehydrated through an ethanol series and embedded in paraffin wax. Sections (thickness, 5 μm) were cut, stained with hematoxylin and eosin, and examined under a light microscope.

2.7. Statistical analysis

BMD, compressive strength, and bone volume were compared between IP-CHA, BMP 5 μg and BMP 20 μg groups using ANOVA, followed by Turkey–Kramer test post test. A P value of <0.05 was considered to indicate statistical significance.

3. Results

3.1. Scanning electron microscopy

After PLA-PEG coating, pore surface and interconnecting channels of the composite were surveyed with a SEM at $\times 100$ (Fig. 1A,C) and $\times 5000$ (Fig. 1B,D) magnification. In original IP-CHA, at $\times 5000$ magnification, boundaries of individual hydroxyapatite particles were clearly visible (Fig. 1B). After PLA-PEG coating, the boundaries became ambiguous, suggesting that the thin PLA-PEG layer covered the entire surface of the pores (Fig. 1D). At $\times 100$ magnification, interconnecting channels were still clearly visible after PLA-PEG coating (Fig. 1A,C).

3.2. Radiographic evaluation

In the defect group, although a minimal amount of new bone was observed at both ends of the defect at 8 weeks, the defect was not repaired, indicating that the defect size was critical in this model. Similarly, in the IP-CHA alone group, small areas at both ends of the implant were radiopaque at 8 weeks, but radiolucent lines were clearly visible between the implant and host bone, suggesting non-union. In contrast, in both 5 μg and 20 μg BMP groups, the entire implant was highly radiopaque at 4 weeks after implantation. In the 5 μg BMP group, a small amount of radiopaque shadow was observed outside the implant, mainly at the junctional sites. In the 20 μg BMP group, a radiopaque shadow up to 2 mm thick covered nearly the entire implant. Eight weeks after implantation, in both BMP 5 and 20 μg groups, the radiodensity of the implants had further increased, and excess newly formed bone outside the

implants had been remodeled to form a smooth repair (Fig. 2). Table 1 summarizes the results of radiographic evaluation. In both BMP groups, all implants showed bilateral union and sclerotic change of the entire implant by 4 weeks after surgery. However, in the IP-CHA alone group, only two implants exhibited unilateral union and none showed sclerotic change (Table 1).

3.3. Histology

Macroscopic appearance of the histological sections was consistent with the findings of radiographic examination. In both BMP groups, at 4 weeks after implantation, almost all pores in the IP-CHA were filled with trabecular bone and hematopoietic marrow. The junctions between the implant and host bone were bony fused, involving new bone formation outside the implant and in the marrow cavity of the bone adjacent to the implant. In the 20 μ g BMP group, prominent bone formation covering almost the entire implant was observed. The newly formed bone observed at 4 weeks outside the implant and in the marrow cavity had

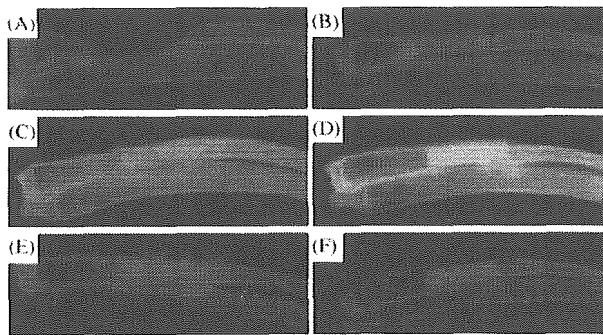


Fig. 2. Soft X-ray photographs. Defect group at 8 weeks after operation (A). IP-CHA alone group at 8 weeks after implantation (B). BMP 5 μ g group: at 4 weeks (C) and 8 weeks (D). BMP 20 μ g group: at 4 weeks (E) and 8 weeks (F). In IP-CHA alone group, radiolucent lines were clearly visible between the implant and host bone, and the radiodensity of the implant had not increased at 8 weeks (B). In the 5 and 20 μ g BMP groups, radiopaque shadows were observed at junctional sites, the entire implant was radiopaque at 4 weeks (C,E), and the radiodensity had further increased at 8 weeks (D,F).

Table 1
Summary of radiographic evaluation

Groups	4 weeks		8 weeks	
	Gain of opacity ^a	Junction with bony union ^b (union/junction)	Gain of opacity	Junction with bony union(union/junction)
IP-CHA alone			0/5	2/10
BMP 5 μ g	5/5	10/10	5/5	10/10
BMP 20 μ g	5/5	10/10	5/5	10/10

^a Number of implants that gained radiopacity.

^b Each implants has two junctions between host bone. These data shows union junction per total junctions (10).

disappeared at 8 weeks, suggesting resorption of excess new bone in remodeling. Interestingly, pores in the outer part of the cylindrical implant were filled predominantly by dense bone matrix like cortical bone, and pores in the central part contained abundant hematopoietic marrow. In contrast, in the IP-CHA group, little bone tissue was found in the pores at both ends of the implants, and most pores were filled with fibrous tissue at 8 weeks after implantation (Fig. 3).

3.4. BMD

In both BMP groups, BMD had increased significantly at 4 weeks after implantation. At 4 weeks, the 20 μ g BMP group had a higher mean BMD than the BMP 5 μ g group. However at 8 weeks after implantation, probably due to remodeling (as indicated by soft X-ray and histology), the BMP 5 and 20 μ g groups had

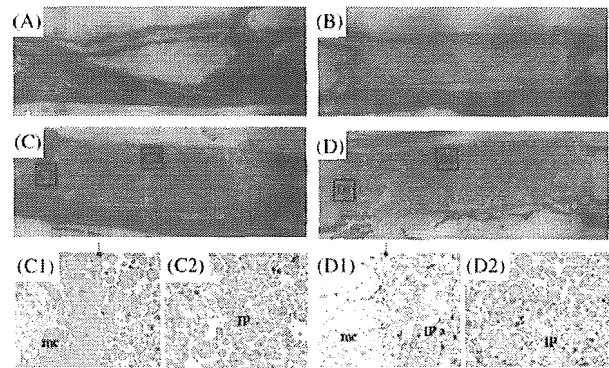


Fig. 3. Low-power photomicrographs of defects: without treatment, at 8 weeks after surgery (A); treated with IP-CHA alone, at 8 weeks (B); BMP 5 μ g group, at 4 weeks (C) and at 8 weeks (D). High-power photomicrographs of 5 μ g BMP group at 4 weeks (C1,C2) and 8 weeks (D1,D2) after surgery. At 4 weeks after surgery, almost all pores in the IP-CHA were evenly filled with trabecular bone and hematopoietic marrow (C2), and newly formed bone was found in the marrow cavity of host bone (C1). At 8 weeks after surgery, an interesting pattern was observed. Pores in the outer part of the cylindrical implant were filled with dense bone matrix, and pores in the center were filled with abundant hematopoietic marrow (D2). Newly formed bone in the marrow cavity was absorbed (D1). mc, marrow cavity; IC, IP-CHA. Arrows indicate implant end (magnification: $\times 40$).

almost the same mean BMD, which was about twice as high as that of the IP-CHA group (Fig. 4).

3.5. Mechanical compression test

The initial breaking load of IP-CHA was approximately 100 N. In the IP-CHA alone group, breaking load did not increase until 8 weeks after implantation. In contrast, in both BMP groups, breaking load steadily increased until 8 weeks after implantation, and the final strength was as high as about 800 N. In both BMP groups, at 4 and 8 weeks after implantation, breaking load was significantly greater than the initial value. There was no significant difference between the BMP groups (Fig. 5).

3.6. Microfocus-CT evaluation

In both BMP groups, mineralized bone matrix newly formed in the porous area of the ceramics was detectable

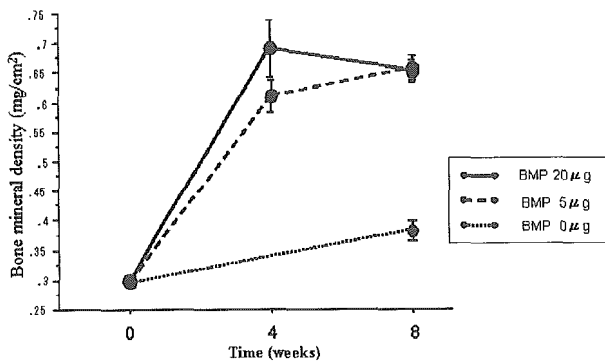


Fig. 4. Bone mineral density of IP-CHA alone group and BMP 5 and 20 µg groups was evaluated by dual-energy X-ray absorptiometry (DXA) using a PIXImus animal densitometer. Each data point represents an average and standard deviation (n = 5).

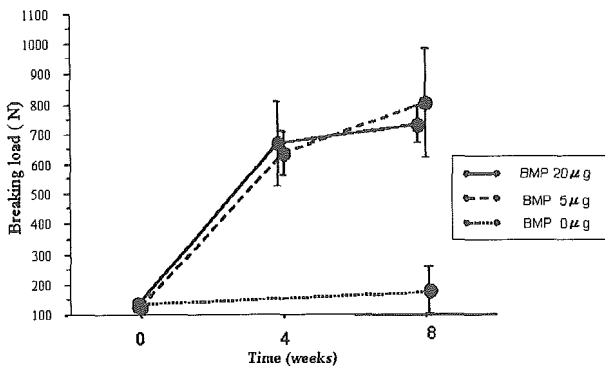


Fig. 5. Breaking load of IP-CHA alone group and BMP 5 and 20 µg groups in compression strength test. Each data point represents an average and standard deviation (n = 4).

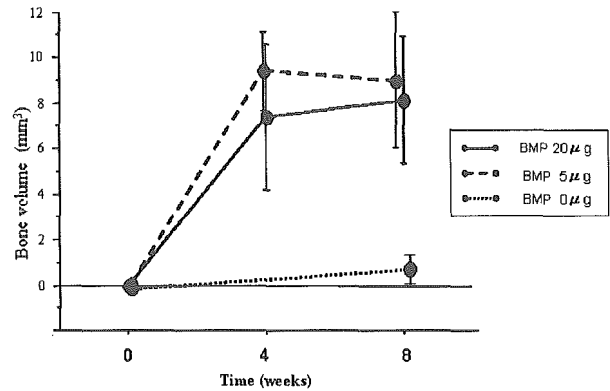


Fig. 6. Bone volume in the pore area of IP-CHA was evaluated using the software package TRI3D-BON (Ratoc System Engineering Co., Ltd., Tokyo, Japan) and the sectional data of the micro-CT image. Each data point represents an average and standard deviation (n = 4).

by microfocus CT at 4 weeks after implantation, and the bone volume in the pores was maintained until 8 weeks after implantation. At 8 weeks, in both BMP groups, bone volume was significantly greater than in the IP-CHA alone group. There was no significant difference in bone volume in the pores between the BMP groups (Fig. 6).

4. Discussion

The present findings demonstrate that a PLA-PEG/IP-CHA composite containing 5 or 20 µg of rhBMP-2 can induce new bone formation in pores and around the implant, leading to complete repair of a critical-size bone defect in rabbit radius with sufficient strength and anatomical structure. Composite containing 5 µg of rhBMP-2 achieved radiographic and histological union at the junctional sites, and the implant gained radiodensity and sufficient mechanical strength. There was a dose-response relationship of rhBMP-2 at 4 weeks after implantation: the higher dose produced superior bone formation around the implant, compared to the lower dose. However, at 8 weeks after surgery, the 5 and 20 µg BMP groups had almost identical radiographic, histological and biomechanical findings. Biomechanically, breaking load of the implant at 8 weeks after surgery was about 800 N, which is almost equal to that of rabbit radius. These findings suggest that PLA-PEG/IP-CHA composite containing 5 µg of rhBMP-2 is sufficient to repair a defect of this size. This dose of BMP is about a tenth of the dose commonly used in previous reports [17–19].

The two biomaterials we combined possess several features that may contribute to the superior ability of the present composite in repair of critical-size segmental bone defects. The interconnected highly porous structure of IP-CHA, with interconnections averaging 40 µm

in diameter, allows efficient migration of bone-producing cells from pore to pore as well as invasion by vascular vessels that is essential for new bone formation. Because IP-CHA combines high porosity and high strength, its three-dimensional structure is preserved whole throughout the repair process, offering an excellent scaffold for bone ingrowth, which apparently facilitates excellent repair of size, shape and mechanical strength. The polymer (PLA-PEG) used in this study is biocompatible and biodegradable, with little inflammatory potential; thus, it does not interfere with new bone formation in the pores. When BMP/PLA-PEG is put in water or implanted *in vivo*, it absorbs water to form a hydrogel, and then degrades gradually and steadily. During this degradation process, BMP is released from the polymer steadily for about 3 weeks. Obviously, the lack of bony repair in the IP-CHA alone group demonstrates the importance of BMP in the repair process, but there is also another factor that seems to be important. Poly D,L-lactic acid-para dioxanone-polyethyleneglycol block co-polymer (PLA-DX-PEG) is reportedly an excellent carrier for rhBMP-2 in a mouse model of ectopic bone formation [5,20]. PLA-DX-PEG, when put in water, releases rhBMP-2 for about 2 weeks. However, in combination with IP-CHA, PLA-DX-PEG/rhBMP-2 composite induces much less bone ingrowth than PLA-PEG/rhBMP-2, which releases BMP-2 for about 3 weeks (data not shown). These findings suggest that the compatibility between scaffolding and BMP-releasing properties of this polymer is another important factor. The optimal combination may vary with factors including implant size, species and local conditions. In addition, swelling of PLA-PEG after absorption of tissue fluid may stabilize the implant and help bone-producing cells to migrate into the implant by filling the gaps between host bone and implant [5,18].

5. Conclusion

This study demonstrated that the composite of PLA-PEG synthetic co-polymer and interconnected porous hydroxyapatite containing only 5 µg of rhBMP-2 completely repaired a critical-size bone defect in rabbit radius with sufficient strength and anatomical structure. Our findings suggest that the combination of these biomaterials potentiates the activity of rhBMP-2 in bone regeneration, leading to a marked reduction of the required amount of rhBMP-2 compared with previous reports.

Acknowledgements

We thank Genetic Institute, Yamanouchi Pharmaceutical Co., Ltd., Taki Chemicals Co., Ltd., and Toshiba Ceramics Co., Ltd., for kindly providing the

chemicals and other materials. We also thank Kaori Asai and Mina Okamoto for their expert technical assistance. This work was supported in part by Grants from the Ministry of Health, Labor and Welfare and Ministry of Education, Culture, Sports, Science and Technology, Japan.

References

- [1] Goldberg VM. Natural history of autografts and allografts. In: Older J, editor. *Bone implant grafting*. London: Springer; 1992. p. 9–12.
- [2] Wozney JM, Rosen V, Celeste AJ, Mitsick LM, Whitters MJ, Kriz RW, Hewick RM, Wang EA. Novel regulators of bone formation: molecular clones and activities. *Science* 1988;242:1528–33.
- [3] Wang EA, Rosen V, D'Alessandro JS, Baudny M, Cordes P, Harada T, Israel DI, Hewick RM, Kerns KM, LaPan P, Luxenberg DP, McQuaid D, Moutsatsos IK, Nove J, Wozney EA. Recombinant human bone morphogenetic protein induces bone formation. *Proc Natl Acad Sci USA* 1990;87:2220–4.
- [4] Urist MR. Bone formation by autoinduction. *Science* 1965; 150:893–9.
- [5] Saito N, Takaoka K. New synthetic biodegradable polymers as BMP carriers for bone tissue engineering. *Biomaterials* 2003; 24:2287–93.
- [6] Miyamoto S, Takaoka K, Okada T, Yoshikawa H, Hashimoto J, Suzuki S, Ono K. Evaluation of polylactic acid homopolymers as carriers for bone morphogenetic protein. *Clin Orthop* 1992;278:274–85.
- [7] Takaoka K, Koezuka M, Nakahara H. Telopeptide-depleted bovine skin collagen as a carrier for bone morphogenetic protein. *J Orthop Res* 1991;9(6):902–7.
- [8] Petite H, Viateau V, Bensaid W, Meunier A, Pollak C, Bourguignon M, Oudina K, Sedel L, Guillemin G. Tissue-engineered bone regeneration. *Nat Biotechnol* 2000;18:959–63.
- [9] Urist MR, Lietze A, Dawson E. β -tricalcium phosphate delivery system for bone morphogenetic protein. *Clin Orthop* 1984; 187:277–80.
- [10] Miyamoto S, Takaoka K, Okada T, Yoshikawa H, Hashimoto J, Suzuki S, Ono K. Polylactic acid-polyethylene glycol block copolymer: a new biodegradable synthetic carrier for bone morphogenetic protein. *Clin Orthop* 1993;294:333–43.
- [11] Takaoka K, Nakahara H, Yoshikawa H, Masuhara K, Tsuda T, Ono K. Ectopic bone induction on and in porous hydroxyapatite combined with collagen and bone morphogenetic protein. *Clin Orthop* 1988;234:250–4.
- [12] Aspenberg P, Lohmander S, Thorngren KG. Monkey bone matrix induces bone formation in the athymic rats, but not in adult monkeys. *J Orthop Res* 1991;9:20–5.
- [13] Miyamoto S, Takaoka K, Ono K. Bone induction in monkeys by bone morphogenetic protein. A trans-filter technique. *J Bone Joint Surg* 1993;75B:107–10.
- [14] Tamai N, Myoui A, Tomita T, Nakase T, Tanaka J, Ochi T, Yoshikawa H. Novel Hydroxyapatite ceramics with an interconnective porous structure exhibit superior osteoconduction *in vivo*. *J Biomed Mater Res* 2002;59(1):110–7.
- [15] Saito N, Okada T, Horiuchi H, Murakami N, Takahashi J, Nawata M, Ota H, Nozaki K, Takaoka K. A biodegradable polymer as a cytokine delivery system for inducing bone formation. *Nat Biotechnol* 2001;19(4):332–5.
- [16] Saito N, Okada T, Horiuchi H, Murakami N, Takahashi J, Nawata M, Ota H, Miyamoto S, Nozaki K, Takaoka K. Biodegradable poly D,L-lactic acid-polyethylene glycol block copolymers as a BMP delivery system for inducing bone. *J Bone Joint Surg* 2001;83-A (Suppl 1)(Part 2):S92–8.

- [17] Kokubo S, Fujimoto R, Yokota S, Fukushima S, Nozaki K, Takahashi K, Miyata K. Bone regeneration by recombinant human bone morphogenetic protein-2 and a novel biodegradable carrier in a rabbit ulnar defect model. *Biomaterials* 2003;24:1643–51.
- [18] Murakami N, Saito N, Horiuchi H, Okada T, Nozaki K, Takaoka K. Repair of segmental defects in rabbit femeri with titanium fiber mesh cylinders containing recombinant human bone morphogenetic protein-2 (RHBMP-2) and a synthetic polymer. *J Biomed Mater Res* 2002;62:169–74.
- [19] Wheeler DL, Chamberland DL, Schmitt JM, Buck DC, Brekke JH, Hollinger JO, Joh SP, Suh KW. Radiomorphometry and biomechanical assessment of recombinant human bone morphogenetic protein 2 and polymer in rabbit radius ostectomy model. *J Biomed Mater Res* 1998;43(4):365–73.
- [20] Murakami N, Saito N, Takahashi J, Ota H, Horiuchi H, Nawata M, Okada T, Nozaki K, Takaoka K. Repair of a proximal femoral bone defect in dogs using a porous surfaced prosthesis in combination with recombinant BMP-2 and synthetic polymer carrier. *Biomaterials* 2003;24:2153–9.

Leptin regulates chondrocyte differentiation and matrix maturation during endochondral ossification

Yuki Kishida^a, Makoto Hirao^a, Noriyuki Tamai^a, Akihide Nampei^a, Tetsuho Fujimoto^a,
Takanobu Nakase^b, Nobuyuki Shimizu^a, Hideki Yoshikawa^a, Akira Myoui^{a,*}

^aDepartment of Orthopaedic Surgery, Osaka University Graduate School of Medicine, 2-2 Yamadaoka, Suita, Osaka 565-0871, Japan

^bDepartment of Orthopaedic Surgery, Osaka National Hospital, Japan

Received 12 January 2005; revised 6 May 2005; accepted 24 May 2005

Available online 20 July 2005

Abstract

Leptin has been suggested to mediate a variety of actions, including bone development, via its ubiquitously expressed receptor (Ob-Rb). In this study, we investigated the role of leptin in endochondral ossification at the growth plate. The growth plates of wild-type and ob/ob mice were analyzed. Effects of leptin on chondrocyte gene expression, cell cycle, apoptosis and matrix mineralization were assessed using primary chondrocyte culture and the ATDC5 cell differentiation culture system. Immunohistochemistry and in situ hybridization showed that leptin was localized in prehypertrophic chondrocytes in normal mice and that Ob-Rb was localized in hypertrophic chondrocytes in normal and ob/ob mice. Growth plates of ob/ob mice were more fragile than those of wild-type mice in a mechanical test and were broken easily at the chondro-osseous junction. The growth plates of ob/ob mice showed disturbed columnar structure, decreased type X collagen expression, less organized collagen fibril arrangement, increased apoptosis and premature mineralization. Leptin administration in ob/ob mice led to an increase in femoral and humeral lengths and decrease in the proportional length of the calcified hypertrophic zone to the whole hypertrophic zone. In primary chondrocyte culture, the matrix mineralization in ob/ob chondrocytes was stronger than that of wild-type mice; this mineralization in both types of mice was abolished by the addition of exogenous leptin (10 ng/ml). During ATDC5 cell differentiation culture, exogenous leptin at a concentration of 1–10 ng/ml (equivalent to the normal serum concentration of leptin) altered type X collagen mRNA expression and suppressed apoptosis, cell growth and matrix calcification. In conclusion, we demonstrated that leptin modulates several events associated with terminal differentiation of chondrocytes. Our finding that the growth plates of ob/ob mice were fragile implies a disturbance in the differentiation/maturation process of growth plates due to depletion of leptin signaling in ob/ob mice. These findings suggest that peripheral leptin signaling plays an essential role in endochondral ossification at the growth plate.
© 2005 Elsevier Inc. All rights reserved.

Keywords: Leptin; Growth plate; Endochondral ossification; ob/ob mouse; Bone chondrocyte differentiation

Introduction

Leptin, a 16-kDa protein encoded by the obese (ob) gene, hormonally regulates food intake and energy expenditure by negative feedback at the hypothalamic nuclei [1]. Leptin is expressed predominantly in adipose tissue of normal mice and is absent in ob/ob mice, which are homozygous for the ob mutation. Leptin is thought to act primarily at the

hypothalamus, where it has effects on appetite, energy expenditure and neuroendocrine axes [2].

Recent studies show that leptin is produced in placenta, skeletal muscle, fetal bone/cartilage and primary cultures of human osteoblasts [3–6]. In addition to its effects on the central nervous system, leptin reportedly exerts effects on cells in peripheral tissues via high-affinity leptin receptors [3–9].

Several reports show that leptin deficiency in humans and mice leads to phenotypic abnormalities in skeletal development, the endocrine system, the immune system and the sympathetic nervous system [10–12]. A human with

* Corresponding author. Fax: +81 6 6879 3559.

E-mail address: myoi@ort.med.osaka-u.ac.jp (A. Myoui).

congenital leptin deficiency reportedly exhibited advanced bone age, indicating abnormalities in bone development [13]. Femora of ob/ob mice are shorter than those of wild-type mice [8]. Linear growth occurs by endochondral bone formation, in which epiphyseal growth plate chondrocytes undergo an organized program of proliferation, maturation, hypertrophic conversion and calcification [14–17]. Thus, the available evidence indicates that leptin has an important function in the growth plate and plays a key role in endochondral ossification. However, there have been few studies of the role of leptin in the regulation of endochondral ossification *in vitro* or *in vivo*.

In the present study, we examined the growth plate cartilage of long bones in ob/ob mice. In addition, we analyzed the effect of leptin on chondrocytic differentiation of *in vitro* using primary chondrocyte culture and murine ATDC5 chondrocytic cell line. The present results suggest that leptin plays an important role in the regulation of physiological processes of endochondral ossification in growth plate cartilage.

Material and methods

Animals

Ob/ob mice were purchased from the Jackson Laboratory (Bar Harbor, ME, USA). All mice were housed under specific pathogen-free conditions with a 12-h light and dark cycle. Intercrossing of heterozygous animals produced homozygous ob/ob mice and wild-type mice. Under anesthesia, 0.5 cm of the tail of each mouse was removed, and genomic DNA was extracted from this material using a DNA mini kit (Qiagen, Valencia, CA, USA). Genotyping was performed using the method of Namae et al. [18]. The housing, care and experimental protocol were approved by the Animal Care and Use Committee of Osaka University.

Measurement of femoral and humeral length

Femora and humeri of 4-week-old wild-type ($n = 10$) and ob/ob mice ($n = 6$) were radiographed and analyzed using Scion Image software (Scion Corporation, Frederick, MD, USA) to determine femoral and humeral length.

Immunohistochemistry and histological analysis

The femora, tibiae and humeri were removed, fixed in 4% paraformaldehyde (Merck, Darmstadt, Germany) in phosphate-buffered saline (PBS, pH 7.4; Sigma, St. Louis, MO, USA), decalcified in 20% EDTA, dehydrated through an ethanol series, embedded in paraffin and then cut into 4- μ m sections. Immunohistochemistry was performed using the streptavidin–peroxidase method with Histofine SAB-PO kits and an aminoethyl carbazole (AEC) substrate kit (Nichirei, Tokyo, Japan) according to the manufactur-

er's protocol. Tissue sections were deparaffinized, hydrated in PBS and incubated in 3% H₂O₂ in methanol for 20 min at room temperature to block endogenous peroxidase activity. After being washed in PBS, the sections were preincubated with 10% normal serum from the same species as the secondary antibody (to minimize background staining) for 20 min at room temperature. Sections were then incubated with two different primary antibodies, anti-leptin polyclonal antibody (Santa Cruz Biotechnology, Santa Cruz, CA, USA) and anti-leptin receptor polyclonal antibody (Santa Cruz Biotechnology) overnight at 4°C. After washing in PBS, the sections were incubated with secondary antibody for 20 min at room temperature. Sections were then incubated with peroxidase-conjugated streptavidin for 20 min at room temperature and washed in PBS. Finally, visualization was performed using AEC as a substrate. As a control for immunostaining, normal serum from the same species as the primary antibodies was used instead of the primary antibodies.

In situ hybridization

A 500-bp leptin fragment and a 450-bp Ob-Rb fragment were cut out and then inserted into pGEM-T easy plasmid (Promega, Madison, WI, USA). The plasmid was linearized with *Nco*I or *Spe*I. Then, *in vitro* transcription and digoxigenin labeling were performed to prepare sense or antisense RNA probes, respectively, using the digoxigenin RNA labeling kit (Roche Diagnostics, Lewes, UK). Paraffin-embedded sections were deparaffinized, rehydrated and heated in 100 mM citric acid buffer in a microwave oven (H2800 Microwave Processor; Energy Beam Sciences, Agawam, MA, USA) at 95°C for 10 min. Then, sections were treated with 1 μ g/ml proteinase K at 37°C for 5 min and treated with 0.2 M HCl for 20 min to quench endogenous alkaline phosphatase. Each section was covered with a single-strand RNA probe and 50 μ l of hybridization solution (Dako Cytomation, Kyoto, Japan) and then incubated at 50°C for overnight. After hybridization, the slides were washed at 50°C. RNaseA treatment (10 μ g/ml) proceeded at 37°C for 20 min. Hybridized signals were detected by a color reaction using 4-nitroblue tetrazolium chloride and 5-bromo-4-chloro-3-indolyl phosphate (Dako).

Mechanical test

Tibiae of 8-week-old wild-type ($n = 10$) and ob/ob ($n = 6$) mice were used. The muscles were removed, and the bones were wrapped with normal saline-soaked gauze. The bones were stored in a plastic bag at -80°C before processing. The distal part of the tibia was embedded in resin (Tray Resin II; Shofu, Kyoto, Japan) and secured so that the load-bearing axis was parallel to the anterior–posterior axis of the proximal growth plate. The proximal epiphysis was loaded with 20 N at 10 mm/min using a testing machine (MZ-500D; Marto, Tokyo, Japan). The